

## States in $^{20}\text{O}$ by use of $^{18}\text{O}(t,p\gamma)$ measurements

K. C. Young, Jr., D. P. Balamuth, J. M. Lind, and R. W. Zurmühle

*Physics Department, University of Pennsylvania, Philadelphia, Pennsylvania 19104*

(Received 22 August 1980)

Levels in  $^{20}\text{O}$  populated in the  $^{18}\text{O}(t,p)^{20}\text{O}$  reaction have been studied at bombarding energies of 10 and 12 MeV using proton- $\gamma$  angular correlation measurements in an axially symmetric geometry. Spin assignments have been made to levels at 1.67 MeV ( $J^\pi = 2^+$ ) and 4.06 MeV ( $J^\pi = 2^+$ ). The angular correlations measured for levels at  $E_x = 4.45$  and 5.38 MeV are consistent with  $J^\pi = 0^+$  for both. The  $E2/M1$  mixing ratio for the 4.06  $\rightarrow$  1.67 MeV transition is measured as  $\delta = -0.18 \pm 0.08$ . Comparison of relative electromagnetic matrix elements (obtained from mixing ratio and branching ratio measurements) with the predictions of shell model calculations suggests that excitations out of the  $1p$  shell play a role in describing these transitions. The population parameters measured for the  $(t,p)$  reaction leading to the first excited states of  $^{18}\text{O}$  and  $^{20}\text{O}$  show that at  $E_t = 12$  MeV the reaction mechanism is predominantly direct.

[ NUCLEAR REACTIONS  $^{18}\text{O}(t,p\gamma)^{20}\text{O}$ ,  $^{16}\text{O}(t,p\gamma)^{18}\text{O}$ ,  $E = 10, 12$  MeV, measured  $\sigma(E_p)$ ,  $p\gamma(\theta)$ ,  $E_\gamma$ .  $^{20}\text{O}$  deduced levels,  $J$ ,  $\pi$ ,  $\delta$ , branching ratios. ]

### 1. INTRODUCTION

Almost all information about excited states in  $^{20}\text{O}$  comes from proton angular distribution measurements using the  $^{18}\text{O}(t,p)^{20}\text{O}$  reaction.<sup>1-5</sup> Because the target nucleus has  $J^\pi = 0^+$ , this reaction also provides a good opportunity to measure  $p$ - $\gamma$  angular correlations. To date, only the 1.67 MeV first excited state has been studied in this way.<sup>6</sup> Such measurements can determine rigorously the spins of the excited states. They are also useful in that, when combined with lifetime measurements, they can determine  $\gamma$ -ray transition rates and thereby serve as a sensitive test for theoretical wave functions describing the states involved. Also, in cases where the spin of a state is known, the  $(t,p\gamma)$  reaction on a spinless target determines the relative populations of the  $M = 0$  and  $M = 1$  magnetic substates in the final state and can thus provide insight into the reaction mechanism. Specifically, in the absence of spin-orbit coupling in the proton or triton optical potentials, any one-step distorted-wave Born approximation (DWBA) calculation involving the transfer of an  $S = 0$ ,  $T = 1$  dineutron will produce a final state which is completely aligned:  $P(0) = 1$ . The present experimental data afford the opportunity to test this prediction in a situation where a direct reaction description is believed to be reasonably accurate. For these reasons, we have measured  $p$ - $\gamma$  angular correlations for excited states of  $^{20}\text{O}$  as part of a series of  $(t,p\gamma)$  measurements on light nuclei.<sup>7,8</sup> In addition, during the measurement of the angular correlation for the first excited state of  $^{20}\text{O}$  the first excited state

of  $^{18}\text{O}$  was studied simultaneously using the  $^{16}\text{O}(t,p\gamma)^{18}\text{O}$  reaction on the  $^{16}\text{O}$  contaminant in the target. [The similar  $Q$  values for the two reactions enabled the limited (10%) dynamic range of the magnetic spectrometer to accept the proton groups from both reactions at the same time.] Consequently, a comparison can also be made between the angular correlations in the two nuclei and the predictions of a direct reaction model for the population parameters. The experimental arrangement and data reduction procedures are discussed in Section 2. The results are summarized in Section 3 and discussed in Section 4, where comparison is made with the prediction of recent shell model calculations.

### 2. EXPERIMENTAL PROCEDURE AND ANALYSIS

Triton beams with intensities between 30 and 150 nA were produced using a Middleton-type negative ion source.<sup>9</sup> They were accelerated to energies of 10 and 12 MeV by the University of Pennsylvania tandem Van de Graaff accelerator. Targets consisted of  $180 \mu\text{g}/\text{cm}^2$   $\text{WO}_3$  (enriched in  $^{18}\text{O}$ ) evaporated onto a  $150 \mu\text{g}/\text{cm}^2$  Au backing. Protons from the  $(t,p)$  reaction were detected at  $0^\circ$  relative to the beam direction using a 10.2 cm long solid-state position-sensitive detector (PSD) which was located in the focal plane of a magnetic spectrometer.<sup>10</sup> Scattered beam particles were stopped by a 0.0025 cm thick Ta foil placed in front of the PSD. Time-coincident  $\gamma$  rays were detected by four NaI(Tl) scintillators placed at  $90^\circ$ ,  $113^\circ$ ,  $136^\circ$ , and  $159^\circ$  relative to the beam at a

distance of 20 cm from the target.

For each  $p\text{-}\gamma$  coincidence event, data consisting of the proton energy ( $E_p$ ) and position ( $P \times E_p$ ),  $\gamma$ -ray energy ( $E_\gamma$ ),  $p\text{-}\gamma$  time difference and routing information were written onto magnetic tape using a PDP-9 computer. Divided  $0^\circ$  position singles and prescaled  $\gamma$  ray singles spectra were recorded in a separate part of each coincidence buffer. Playback and analysis of the data were done off-line using the same computer. The resulting  $p\text{-}\gamma$  angular correlations were fitted using the computer program M2.<sup>11</sup>

The axially symmetric geometry of the present experiment and conservation of angular momentum require that the alignment of the  $^{20}\text{O}$  nuclei formed in this reaction is completely described by the fraction in the  $M = 0$  and  $|M| = 1$  magnetic substates. Assuming that the  $(t,p)$  reaction at these energies proceeds by the direct transfer of an  $S = 0$ ,  $T = 1$  dineutron (and neglecting spin-orbit coupling), only the  $M = 0$  substate can be populated. In the initial analysis of the angular correlations, the parameter  $P(0)$  describing the alignment of the final state was treated as a free parameter. However, as discussed below, if this procedure did not uniquely identify a spin, the population parameters were restricted to the most probable range near  $P(0) = 1$  in a second analysis of the angular correlation.

### 3. EXPERIMENTAL RESULTS

The angular correlation measurements were made at  $E_i = 10$  MeV for the  $E_x = 4.06$  and 4.45 MeV states and at  $E_i = 12$  MeV all other states. The results of the angular correlation analysis are summarized in Table I.

#### A. 1.67 MeV state

The angular correlation for the first excited state in  $^{20}\text{O}$  rigorously determines the spin of the state as  $J = 2$ ; other spins are ruled out with better than 99.9% confidence. Since this state has a reasonably large cross section in the  $(t,p)$  reaction, we assume natural parity, i.e.  $J^\pi = 2^+$ . This result is in agreement with previous assignments from angular correlation<sup>6</sup> and angular distribution<sup>1-5</sup> measurements.

The proximity of the proton group leading to the first excited state of  $^{18}\text{O}$  enabled the angular correlation for the  $^{16}\text{O}(t,p\gamma)^{18}\text{O}$  reaction to be obtained simultaneously with that for the 1.67 MeV level in  $^{20}\text{O}$ . Given that both final states have  $J^\pi = 2^+$ , the angular correlations determine the population parameters  $P(M)$  for  $|M| = 0, 1$ . Both angular correlations are shown in Fig. 1, along with the best fits obtained (solid curves). The angular correlations are qualitatively similar; their shape is characteristic of the expected dominance of the  $M = 0$  magnetic substate. Quantitatively there are differences between the two:

TABLE I. Angular correlation results.

Transition ( $E_i \rightarrow E_f$ )	$J_i$	$\delta^a$	$P(0)$	$\frac{\chi^2}{\nu}$
1.67 $\rightarrow$ 0	1		0.0 <sup>b</sup>	31.0
	2		$0.80 \pm 0.04$	0.4
	3		$0.15 \pm 0.06$	17.7
4.06 $\rightarrow$ 0	1		0.0	110.0
	2		1.0 <sup>b</sup>	2.48
	3		0.0	48.7
4.06 $\rightarrow$ 1.67 $\rightarrow$ 0	0		1.0	24.7
	1	$-1.71^{+0.41}_{-0.63}$	0.0 <sup>b</sup>	25.8
	2	$-0.18 \pm 0.08$	1.0 <sup>b</sup>	0.94
	3	$2.76^{+0.45}_{-0.62}$	1.0 <sup>b</sup>	11.0
4.45 $\rightarrow$ 1.67 $\rightarrow$ 0	4	$-8.11^{+2.87}_{-3.46}$	$0.94 \pm 0.18$	8.9
	0		1.0	2.3
	1	$0.18 \pm 0.16$	$0.56 \pm 0.12$	2.5
	2	$0.31 \pm 0.10$	$0.46 \pm 0.08$	2.4
5.38 $\rightarrow$ 1.67 $\rightarrow$ 0	3	$0.07 \pm 0.09$	0.0 <sup>b</sup>	2.8
	4	$2.91^{+1.32}_{-0.73}$	0.0 <sup>b</sup>	4.0
	0		1.0	1.2
	1	$-0.28 \pm 0.34$	$0.46 \pm 0.10$	1.3
	2	$0.48 \pm 0.14$	$0.35 \pm 0.10$	1.6
	3	$0.30 \pm 0.19$	0.0 <sup>b</sup>	1.6
	4	$2.42^{+1.16}_{-0.64}$	0.0 <sup>b</sup>	5.5

<sup>a</sup> Phase convention of Rose and Brink (Ref. 18).

<sup>b</sup> Best fit gave unphysical value for  $P(0)$ —nearest physical value used.

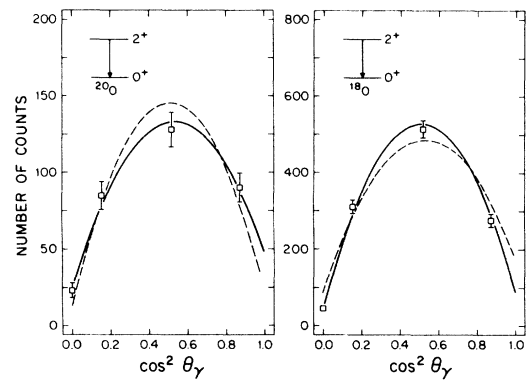


FIG. 1. Angular correlations for the decay of the first excited state of  $^{20}\text{O}$  (left) and  $^{18}\text{O}$  (right). The solid curves are the best fits; the dashed lines show the same curves interchanged, as described in the text.

the angular correlation in  $^{20}\text{O}$  is noticeably less anisotropic than in  $^{18}\text{O}$ . This is illustrated in Fig. 1, where the data have simply been fitted treating the substate populations as free parameters. The best fit is shown as a solid curve in each case; the best fit for  $^{18}\text{O}$  is shown as a dashed curve with the  $^{20}\text{O}$  data and vice versa.

Before these differences are interpreted in terms of the nuclear reaction mechanism populating the respective states, however, a correction must be applied for possible perturbation of the angular correlation by the hyperfine interaction between the nuclear spin and unpaired  $2s$  electrons in the electronic configuration of the recoiling atom. Such effects have been shown to be important<sup>12</sup> even in cases such as the present one where the recoil velocity is low and the residual excited nuclei emerge in states of low ionization. An estimate of the required correction was made by assuming than an effective hyperfine field  $H(0)$  of 5 MG (see Table 2 of Ref. 12) is experienced by all the recoiling nuclei. The time-integrated attenuation coefficients  $G_k$  were then obtained from

$$G_k = 1 - \frac{k(k+1)(\omega\tau)^2}{(2I+1)^2(1+(\omega\tau)^2)}$$

This prescription results in a negligible correction for  $^{18}\text{O}$ ; for  $^{20}\text{O}$  the longer lifetime and larger  $g$  factor (see Ref. 13) yields correction factors  $G_2 = 0.96$  and  $G_4 = 0.86$ . After correcting for the effects of attenuation in this way, the resulting population parameters for the  $M = 0$  magnetic substate are found to be  $P(0) = 0.866 \pm 0.057$  in  $^{20}\text{O}$  and  $P(0) = 0.920 \pm 0.017$  in  $^{18}\text{O}$ . (The smaller error for  $^{18}\text{O}$  mainly reflects better statistics; in the case of  $^{20}\text{O}$  a 20% uncertainty in  $\omega\tau$  was assumed in calculating the hyperfine field corrections.)

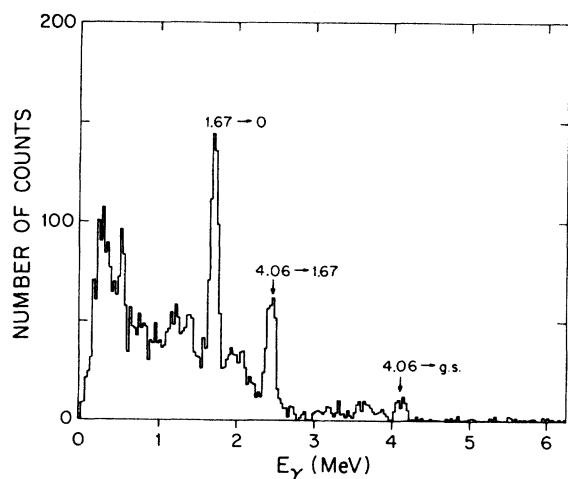


FIG. 2. Gamma spectrum for the decay of the  $E_x = 4.06$  MeV level.

### B. 4.06 MeV state

Figure 2 shows a four crystal  $\gamma$  sum spectrum for the decay of the 4.06 MeV state. It indicates that the level decays to both the ground ( $26 \pm 4\%$ ) and first excited ( $74 \pm 4\%$ ) states. The angular correlations for both the ground state decay (Figure 3) and the cascade through the 1.67 MeV state (Figure 4) provide a  $J = 2$  assignment for this level. Again, the reaction strength favors natural parity. The angular correlation determines the  $E2/M1$  mixing ratio for the  $2^+$  to  $2^+$  transition as  $\delta = -0.18 \pm 0.08$ . Previous angular distribution measurements<sup>1-5</sup> also indicated  $J^\pi = 2^+$  for this level.

### C. 4.45 MeV state

The  $\gamma$ -ray spectrum shown in Figure 5 indicates that this level decays primarily through the 1.67 MeV first excited state. We place an upper limit of 4% on a branch to the ground state. The angular correlations for the  $4.45 \rightarrow 1.67 \rightarrow \text{g.s.}$  decay sequence are shown in Figure 6. It was not possible to make a rigorous spin assignment for this state from a fit to

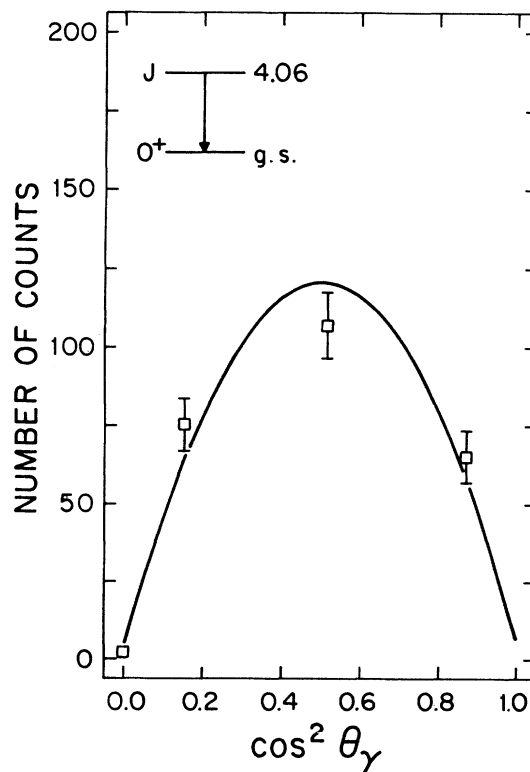


FIG. 3. Angular correlation for the ground state decay of the 4.06 MeV level. The curve is a fit assuming  $J = 2$ .

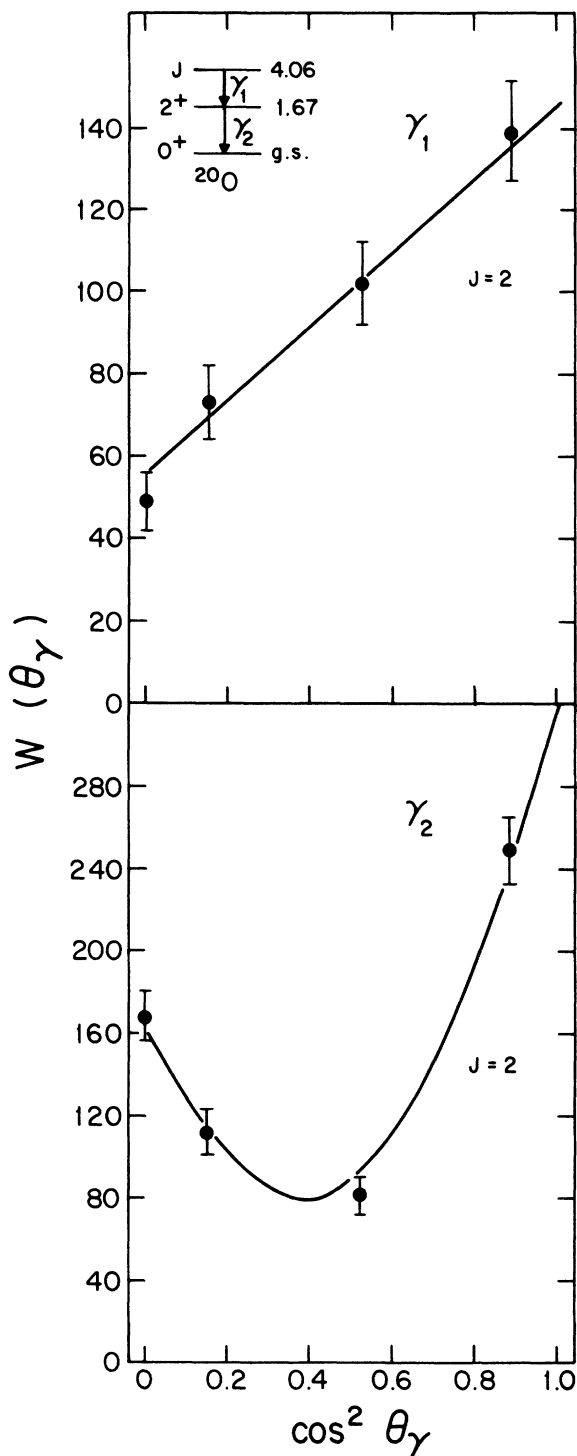


FIG. 4. Angular correlations for the cascade decay of the 4.06 MeV level through the first excited state.

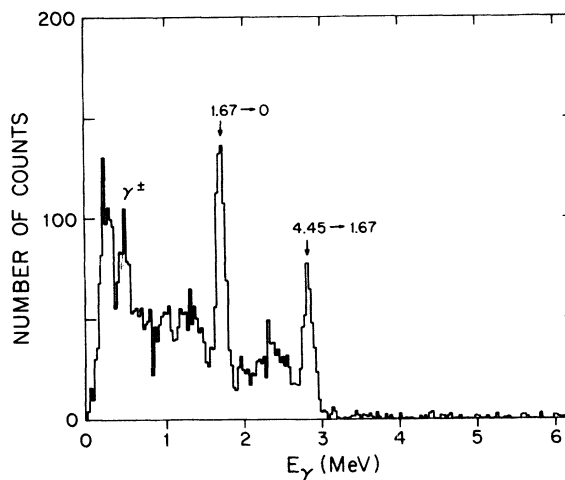


FIG. 5. Gamma spectrum for the decay of the  $E_x = 4.45$  MeV level.

the experimental angular correlation (see Table I). Previous angular distribution measurements<sup>1,4,5</sup> suggested spin and parity  $0^+$  for this state, and the essentially isotropic angular correlation obtained in this study supports such an assignment. To provide further support for the  $J = 0$  hypothesis,  $\chi^2/\nu$  values were determined assuming  $P(0) = 0.8$  for  $J$  values between 1 and 4.  $P(0) = 0.8$  was chosen somewhat arbitrarily to accommodate possible compound nuclear contributions to the reaction mechanism. These results are shown in Table II. Again, it is not possible to exclude all other spins from this analysis, but fits with  $J=3,4$  have  $\chi^2/\nu$  values above the 0.1% confidence level. Thus, we favor  $J^\pi = 0^+$  for the 4.45 MeV level but cannot rule out  $J = 1-3$ .  $J = 4$  is unlikely because of the poor fit and the large mixing ratio which would be required for the primary  $\gamma$  ray.

TABLE II. Angular correlation fits with constrained  $P(0) = 0.8$ . See text.

Transition ( $E_i \rightarrow E_f$ )	$J_i$	$\frac{\chi^2}{\nu}$
4.45 $\rightarrow$ 1.67 $\rightarrow$ 0	1	2.7
	2	4.7
	3	8.1
	4	8.5
5.38 $\rightarrow$ 1.67 $\rightarrow$ 0	1	2.8
	2	4.3
	3	7.2
	4	9.3

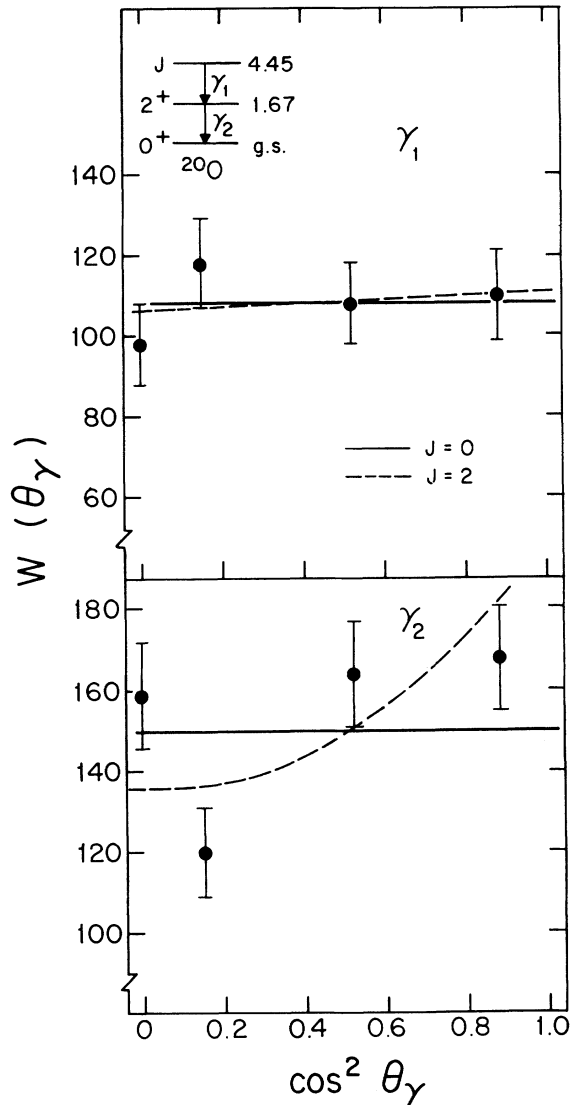


FIG. 6. Angular correlations for the cascade decay of the 4.45 MeV level through the first excited state.

#### D. 5.38 MeV state

Figure 7 shows the  $\gamma$  decay spectrum for the 5.38 MeV level and indicates that it decays primarily through the 1.67 MeV state. The ground state branch is less than 7%. The fits to the  $\gamma$ -ray angular correlations shown in Figure 8 rule out  $J = 4$ , but cannot distinguish between  $J = 0, 1, 2$ , or 3 as indicated in Table I. Again, the isotropic angular correlation is consistent with  $J^\pi = 0^+$  for this state and such an assignment would be in agreement with previous angular distribution measurements.<sup>5</sup> Fixing  $P(0) = 0.8$  results in the  $\chi^2/\nu$  values shown in Table

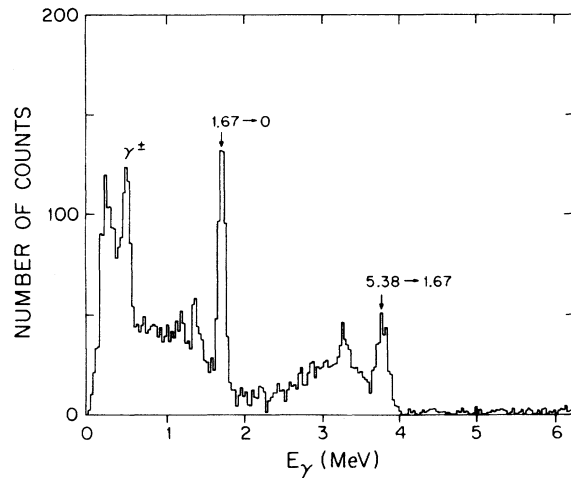


FIG. 7. Gamma spectrum for the decay of the  $E_x = 5.38$  MeV level.

II and provide further support for the  $J^\pi = 0^+$  assignment.

#### E. Other weak states

States at  $E_x = 5.22$  and 5.29 MeV were also observed during the run on the 5.38 MeV level. However, the cross sections at  $E_i = 12$  MeV were so small that angular correlation measurements were not practical. Gamma ray spectra with rather poor statistics indicate that the 5.22 MeV level decays through the first excited state. A tentative  $J = (1^-, 2^+)$  assignment has been made to this level.<sup>4</sup> We are unable to choose between these possibilities. The 5.29 MeV state appears to decay through the first excited state and also to the ground state.

#### F. Population parameter measurements

In order to compare the measured population parameters with theory, the  $M$ -state populations predicted by the DWBA were calculated using the program DWUCK4.<sup>14</sup> Optical model potentials describing the triton and proton distorted waves were taken from the work of La France *et al.*,<sup>5</sup> who studied the same reaction at a bombarding energy of 15 MeV. The parameters used give a good fit to the measured  $(t,p)$  angular distributions. The same parameters were used for  $^{16}\text{O}(t,p)^{18}\text{O}$ . Reaction amplitudes generated by DWUCK4 were used as input to a computer program which calculates the particle-gamma angular correlation. The finite angular acceptance of the magnetic spectrometer was accounted for

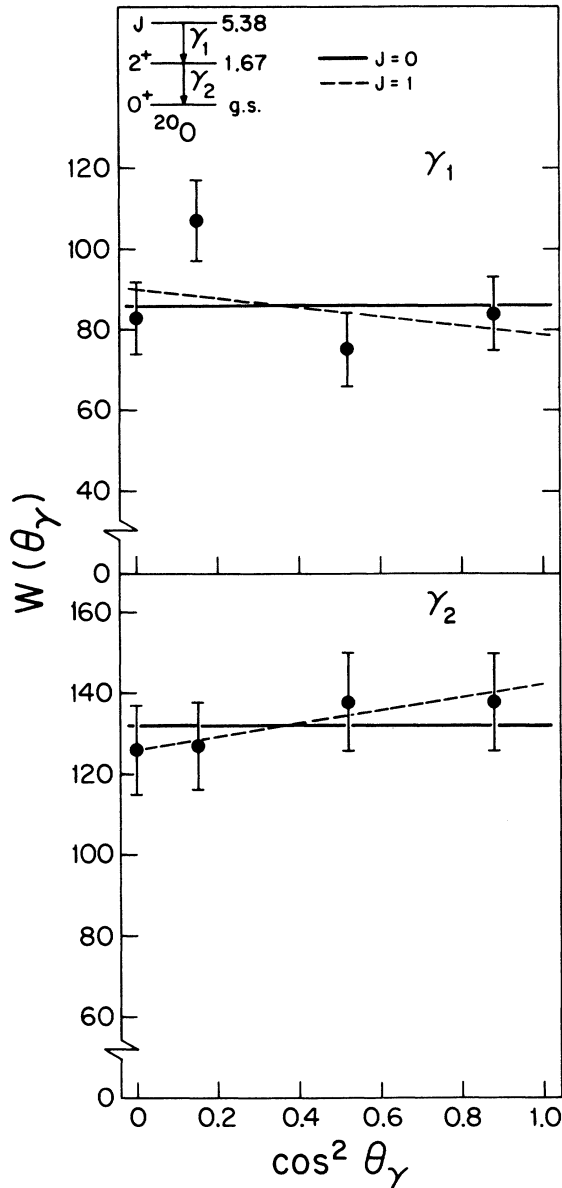


FIG. 8. Angular correlations for the cascade decay of the 5.38 MeV level through the first excited state.

by numerically integrating the calculated angular correlation over a 25 point grid. In this way the contributions of the reaction amplitudes with nonzero values of  $m_l$  are included. The predicted value of  $P(0)$  for the  $^{20}\text{O}$  first excited state is 0.981. Doubling the proton spin-orbit strength changes this prediction to 0.967. Other small changes in optical model parameters also produced negligible changes in the predicted value. The DWBA predictions are to be compared with the present experimental values of  $P(0) = 0.920 \pm 0.017$  and  $P(0) = 0.866 \pm 0.057$  for

$^{18}\text{O}$  and  $^{20}\text{O}$ , respectively. The measurements in the two nuclei agree within their estimated errors; a weighted average gives  $P(0) = 0.915 \pm 0.016$ , which is somewhat less than the DWBA prediction. Given the amount and quality of data in the present experiment, this difference is probably not significant. If the discrepancy were to be accounted for by the admixture of compound nuclear (CN) contributions to the reaction mechanism, approximately 20% of the differential cross section at zero degrees would result from CN processes, assuming that the CN mechanism populates all allowed substates equally.

#### 4. DISCUSSION

It is of some interest to compare the new information obtained on relative electromagnetic transition rates in  $^{20}\text{O}$  with the results of recent shell model calculations. Wildenthal *et al.*<sup>15</sup> and Brown<sup>16</sup> have each performed shell model calculations for  $^{20}\text{O}$  using two different model spaces: (a) four particles are distributed in the  $2s-1d$  shell outside a closed  $^{16}\text{O}$  core; and (b) 8 particles are allowed to occupy the  $1p_{1/2}$ ,  $2s_{1/2}$ , and  $1d_{5/2}$  orbits outside a closed  $^{12}\text{C}$  core. These calculations will be referred to henceforth as  $(sd)^4$  and  $(psd)$  respectively. The calculations of Wildenthal *et al.* and those of Brown gave equivalent results; for convenience in the following we will compare our experimental results with Ref. 16. In these calculations the two-body effective interaction was that of Reehal and Wildenthal; for calculating the electromagnetic matrix elements effective charges  $e_p = 1.35e$ ,  $e_n = 0.35e$  were used, and free nucleon  $g$  factors were assumed.

We begin by considering the decays of the second excited  $2^+$  state at  $E_x = 4.06$  MeV. The new experimental information obtained for this level is the  $E2/M1$  mixing ratio for the transition to the first excited state and the relative branching ratio for this decay and the ground state transition. Since the lifetime of the second  $2^+$  state is not known, only ratios of matrix elements can be compared. Table III shows the comparisons which can be made. Agreement between experiment and theory is clearly better for

TABLE III. Comparison of ratios of matrix elements involved in the decay of the second  $2^+$  state with shell model predictions.

Quantity	$(sd)^4$	$(psd)$	Experiment
$\delta(E2/M1)$	+0.024	-0.055	$-0.18 \pm 0.08$
$\frac{T_{E2}(2_2^+ \rightarrow 0_1^+)}{T_{E2}(2_2^+ \rightarrow 2_1^+)}$	271	4.3	$11^{+24}_6$

the (*psd*) calculation, indicating the importance of excitations out of the  $^{16}\text{O}$  core. (In the case of the (*psd*) calculation, neglecting the  $1d_{3/2}$  state is certainly a problem, but at least for this particular ratio of *E2* transitions a calculation including only the  $2s_{1/2}$  and  $1d_{5/2}$  orbits yields only a factor of 4 reduction in the ratio, compared to the factor of 63 obtained with the (*psd*) calculation.)

A second point of comparison between experiment and theory is the decays of the excited  $0^+$  states at  $E_x = 4.45$  and  $5.38$  MeV. Only one excited  $0^+$  state is predicted near this energy in the (*sd*)<sup>4</sup> model; the calculated excitation energy is  $4.75$  MeV. Based on an analysis of the two-particle transfer cross sections, La France *et al.* (Ref. 5) suggest that the lower excited  $0^+$  state at  $E_x = 4.45$  MeV is predominantly core-excited (6p-2h); the third  $0^+$  state at  $E_x = 5.38$  MeV is identified with the state predicted by the (*sd*)<sup>4</sup> calculation.

In the (*sd*)<sup>4</sup> calculation, the predicted *E2* matrix element connecting the second  $0^+$  and first  $2^+$  levels is very small. This transition is, however, strongly favored over the competing *E2* transition to the second  $2^+$  state by the kinematic factor involving the fifth power of the gamma ray energy. For  $\gamma$  ray energies corresponding to  $E_x = 5.38$  MeV for the second  $0^+$  level these effects essentially cancel and approximately equal branches to the two  $2^+$  states are predicted. Experimentally, only the transition to the lowest  $2^+$  state is observed; an upper limit of 8% may be placed on the transition  $5.38$  MeV  $\rightarrow$   $4.06$  MeV from the present work (see Fig. 7). The experimental ratio of  $B(E2)$ 's connecting the second  $0^+$  level to the first two  $2^+$  states is thus about ten times larger than the prediction from the (*sd*)<sup>4</sup> calculation. This problem is not present in the (*psd*) calculation, which predicts two excited  $0^+$  states at approximately the observed energies, both of which have dominant decay branches to the first excited state. Unfortunately, while the (*psd*) calculation gives a better account of the *E2* transitions, it cannot account for the observed (*t,p*) strengths, predicting a yield to the  $E_x = 4.45$  MeV level about half as large as that to the ground state. (Experimentally the  $4.45$  MeV state has only about 10% of the ground state strength.<sup>5</sup>)

A crude estimate of whether the *E2* decays of the

$5.38$  MeV level can be reconciled with the (*t,p*) strengths of Ref. 5 has been made by Bland and Fortune.<sup>17</sup> The core excited levels were described by weak coupling  $^{22}\text{Ne}$  to  $^{14}\text{C}$  as in Ref. 5. The diagonal matrix elements were taken from the calculated energies for the (*sd*)<sup>4</sup> states and from weak coupling for the core-excited states. The required off-diagonal matrix elements connecting the 6p-2h states to the (*sd*)<sup>4</sup> states were varied about reasonable values (approximately  $1$  MeV) in an attempt to fit the *E2* transitions, the energy levels, and the (*t,p*) strengths. The calculations show that it is indeed possible to mix the 6p-2h and (*sd*)<sup>4</sup> states in such a way that the second  $0^+$  to first  $2^+$  *E2* strength is increased by about a factor of five while still preserving the fact that the (*t,p*) cross sections leading to the two excited  $0^+$  states are different by about a factor of 8 (in agreement with experiment). This suggests that the conclusions of Ref. 5 are qualitatively correct, but that the present data on *E2* rates are more sensitive to core excitation than the (*t,p*) cross sections.

Summarizing, the limited comparison which can be made of the results of the present work with shell model calculations suggests that it is important to treat excitations of particles from the  $1p$  to the  $2s-1d$  shell in order to describe electromagnetic transitions accurately. Also, the hypothesis suggested in Ref. 5 that the observed  $0^+$  state at  $E_x = 5.38$  MeV corresponds literally to the second  $0^+$  state in the (*sd*)<sup>4</sup> model produces results in disagreement with experiment, suggesting a small amount of mixing between 6p-2h and (*sd*)<sup>4</sup> states. This mixing does not seem to be very well described by the (*psd*) calculation, however. More experimental work would be welcome here, in particular lifetime measurements which would enable absolute (as opposed to relative) electromagnetic transition strengths to be determined.

#### ACKNOWLEDGMENTS

We express our thanks to B. H. Wildenthal and to B. A. Brown for communicating the results of their shell model calculations and for illuminating conversations. We are also grateful to H. T. Fortune for stimulating discussions.

1 S. Hinds, H. Marchant, and R. Middleton, Nucl. Phys. **38**, 81 (1962).  
 2 R. Middleton and D. J. Pullen, Nucl. Phys. **70**, 293 (1965).  
 3 R. Moreh, Nucl. Phys. **70**, 293 (1965).  
 4 A. A. Pilt, M. A. M. Shahabuddin, and J. A. Kuehner, Phys. Rev. C **19**, 20 (1979).  
 5 S. LaFrance, H. T. Fortune, S. Mordechai, and R. Middleton, J. Phys. G **5**, L59 (1979).

6 R. W. Nightingale, J. A. Becker, R. E. McDonald, and D. Kohler, Phys. Rev. C **1**, 893 (1970).  
 7 D. E. Alburger, D. P. Balamuth, J. M. Lind, L. Mulligan, K. C. Young, Jr., R. W. Zurmühle, and R. Middleton, Phys. Rev. C **17**, 1525 (1978).  
 8 D. P. Balamuth, J. M. Lind, K. C. Young, Jr., and R. W. Zurmühle, Nucl. Phys. A **290**, 65 (1977).  
 9 R. Middleton and C. T. Adams, Nucl. Instrum. Methods **118**, 329 (1974).

- <sup>10</sup>R. W. Zurmühle, P. F. Hinrichsen, C. M. Fou, C. R. Gould, and G. P. Anastassiou, Nucl. Instrum. Methods 71, 311 (1969).
- <sup>11</sup>D. J. Church (unpublished).
- <sup>12</sup>C. Broude, M. B. Goldberg, G. Goldring, M. Hass, M. J. Renan, B. Sharon, Z. Shkedi, and D. F. H. Start, Nucl. Phys. A 215, 617 (1973).
- <sup>13</sup>Z. Berant, C. Broude, G. Engler, M. Hass, R. Levy, and B. Richter, Nucl. Phys. A 243, 519 (1975).
- <sup>14</sup>P. D. Kunz (unpublished).
- <sup>15</sup>B. H. Wildenthal (private communication).
- <sup>16</sup>B. A. Brown (private communication).
- <sup>17</sup>L. Bland and H. T. Fortune (unpublished).
- <sup>18</sup>H. J. Rose and D. M. Brink, Rev. Mod. Phys. 39, 306 (1967).